Scale-Invariant Continuous Entanglement Renormalization of a Chern Insulator (Supplemental Material)

Su-Kuan Chu,[1,2] Guanyu Zhu,[1] James R. Garrison,[1,2] Zachary Eldredge,[1,2]
Ana Valdés Curiel,[1] Przemyslaw Bienias,[1] I. B. Spielman,[1] and Alexey V. Gorshkov[1,2]
[1]*Joint Quantum Institute, NIST/University of Maryland, College Park, Maryland 20742, USA*
[2]*Joint Center for Quantum Information and Computer Science, NIST/University of Maryland, College Park, Maryland 20742, USA*

In this Supplemental Material, we provide details on scale invariance as well as the experimental realization. In Section I, we show that the wavefunction $|\Psi\rangle$ in Eq. (4) in the main text remains scale-invariant under our cMERA quantum circuit in the Schrödinger picture. In Section II, we show how to engineer a synthetic selection rule between dressed states in the absence of any good quantum number. With that technique in mind, we show a scheme to realize the cMERA circuit in Section III. After that, in Section IV, we provide one way to prepare the initial state for the cMERA circuit by using spatial light modulators [S1, S2].

I. SCALE INVARIANCE OF THE WAVEFUNCTION IN THE SCHRÖDINGER PICTURE

In this section, we demonstrate explicitly that the wavefunction $|\Psi\rangle$ described by Eq. (4) in the main text is actually scale-invariant under the cMERA quantum circuit in the Schrödinger picture. Notice that the wavefunction can also be defined as the wavefunction satisfying

$$\left(u_{\mathbf{k}}\psi_2^\dagger(\mathbf{k})-v_{\mathbf{k}}\psi_1^\dagger(\mathbf{k})\right)|\Psi\rangle=0,\ \forall\,\mathbf{k}. \tag{S1}$$

Under a small time δu, the transformed wavefunction $e^{-i\,\delta u(L+K)}|\Psi\rangle$ is governed by the equation

$$e^{-i\,\delta u(L+K)}\left(u_{\mathbf{k}}\psi_2^\dagger(\mathbf{k})-v_{\mathbf{k}}\psi_1^\dagger(\mathbf{k})\right)e^{+i\,\delta u(L+K)}\left(e^{-i\,\delta u(L+K)}|\Psi\rangle\right)=0,\ \forall\,\mathbf{k}. \tag{S2}$$

Note that

$$\begin{aligned}
&e^{-i\,\delta u(L+K)}\left(u_{\mathbf{k}}\psi_2^\dagger(\mathbf{k})-v_{\mathbf{k}}\psi_1^\dagger(\mathbf{k})\right)e^{+i\,\delta u(L+K)}\\
\approx&\left(u_{\mathbf{k}}\psi_2^\dagger(\mathbf{k})-v_{\mathbf{k}}\psi_1^\dagger(\mathbf{k})\right)-i\,\delta u\left[L+K,u_{\mathbf{k}}\psi_2^\dagger(\mathbf{k})-v_{\mathbf{k}}\psi_1^\dagger(\mathbf{k})\right]\\
=&\left(u_{\mathbf{k}}\psi_2^\dagger(\mathbf{k})-v_{\mathbf{k}}\psi_1^\dagger(\mathbf{k})\right)-\delta u\Big[u_{\mathbf{k}}\left(1+\mathbf{k}\cdot\nabla_{\mathbf{k}}\right)\psi_2^\dagger(\mathbf{k})-v_{\mathbf{k}}\left(1+\mathbf{k}\cdot\nabla_{\mathbf{k}}\right)\psi_1^\dagger(\mathbf{k})-\underbrace{\left(g(\mathbf{k})\,u_{\mathbf{k}}\psi_1^\dagger(\mathbf{k})-g^*(\mathbf{k})\,v_{\mathbf{k}}\psi_2^\dagger(\mathbf{k})\right)}_{=\mathbf{k}\cdot\nabla_{\mathbf{k}}u_{\mathbf{k}}\psi_2^\dagger(\mathbf{k})-\mathbf{k}\cdot\nabla_{\mathbf{k}}v_{\mathbf{k}}\psi_1^\dagger(\mathbf{k})}\Big]\\
\approx&e^{-\delta u}\left(u_{\mathbf{k}e^{-\delta u}}\psi_2^\dagger(\mathbf{k}e^{-\delta u})-v_{\mathbf{k}e^{-\delta u}}\psi_1^\dagger(\mathbf{k}e^{-\delta u})\right).
\end{aligned} \tag{S3}$$

Therefore, we can see that Eq. (S2) is nothing but Eq. (S1) after a change of variable $\mathbf{k}\to\mathbf{k}\,e^{-\delta u}$. In other words, $e^{-i\,\delta u(L+K)}|\Psi\rangle=|\Psi\rangle$.

II. SYNTHETIC SELECTION RULES

In this section, we introduce a trick that will be useful for engineering the disentangler in a real atomic system. Suppose that we have a three-level system composed of states $|s_1\rangle$, $|s_2\rangle$, and $|g\rangle$. In the presence of an on-resonance driving with Rabi frequency Ω between bare states $|s_1\rangle$ and $|s_2\rangle$, two dressed states $|d_1\rangle$ and $|d_2\rangle$ are formed. We are going to show that by fine-tuning the Rabi frequencies χ_1 and χ_2, we can generate a synthetic selection rule from state $|g\rangle$ to the two dressed states $|d_1\rangle$ and $|d_2\rangle$, e.g., $|g\rangle\to|d_2\rangle$ is allowed while $|g\rangle\to|d_1\rangle$ is forbidden. (Once we prove this, the converse case where $|g\rangle\to|d_1\rangle$ is allowed and $|g\rangle\to|d_2\rangle$ is forbidden is a trivial generalization.) We consider a driving Hamiltonian, which under rotating wave approximation is

$$h=\begin{pmatrix}0&\chi_1^*e^{i(\omega_1-\Omega+\delta)t}&\chi_2^*e^{i(\omega_2-\Omega+\delta)t}\\ \chi_1e^{-i(\omega_1-\Omega+\delta)t}&\omega_1&\Omega e^{-i(\omega_1-\omega_2)t}\\ \chi_2e^{-i(\omega_2-\Omega+\delta)t}&\Omega e^{i(\omega_1-\omega_2)t}&\omega_2\end{pmatrix}. \tag{S4}$$

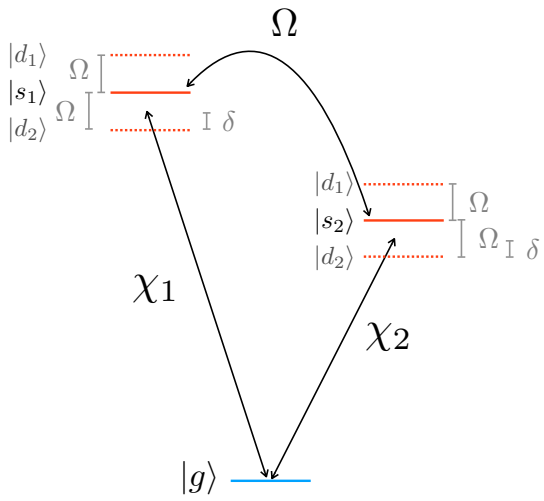

FIG. S1. A toy model of synthetic selection rules. Bare states $|s_1\rangle$ and $|s_2\rangle$ are driven by a field with Rabi frequency Ω, whereby two dressed states $|d_1\rangle$ and $|d_2\rangle$ are created. In view of the rotating frame, the dressed states are linear combinations of bare states. As a result, they do not have good quantum numbers to constitute a selection rule when coupling to another state, say $|g\rangle$. A synthetic selection rule can be generated through applying two driving fields from $|g\rangle$ to $|s_1\rangle$ and $|s_2\rangle$ with fine-tuned Rabi frequencies χ_1 and χ_2, respectively. For example, we can forbid the transition from $|g\rangle$ to $|d_1\rangle$ by choosing $\chi_1 = -\chi_2$.

The order of the columns (rows) is $|g\rangle$, $|s_1\rangle$, $|s_2\rangle$. We have assumed that $|\omega_1 - \omega_2| \gg \Omega$, allowing us to neglect some transitions that are far off-resonant. The level diagram is illustrated in FIG. S1.

Going to the rotating frame defined by the unitary matrix

$$U = \begin{pmatrix} 1 & 0 & 0 \\ 0 & e^{-i(\omega_1-\omega_2)t} & 0 \\ 0 & 0 & 1 \end{pmatrix}, \tag{S5}$$

we obtain the effective Hamiltonian

$$U^\dagger h U - i\partial_t U^\dagger U = \begin{pmatrix} 0 & \chi_1^* e^{i(\omega_2-\Omega+\delta)t} & \chi_2^* e^{i(\omega_2-\Omega+\delta)t} \\ \chi_1 e^{-i(\omega_2-\Omega+\delta)t} & \omega_2 & \Omega \\ \chi_2 e^{-i(\omega_2-\Omega+\delta)t} & \Omega & \omega_2 \end{pmatrix}. \tag{S6}$$

After diagonalizing the 2×2 block on the bottom right, we obtain the following Hamiltonian:

$$\begin{pmatrix} 0 & \frac{1}{\sqrt{2}}(\chi_1^* + \chi_2^*)e^{i(\omega_2-\Omega+\delta)t} & \frac{1}{\sqrt{2}}(\chi_1^* - \chi_2^*)e^{i(\omega_2-\Omega+\delta)t} \\ \frac{1}{\sqrt{2}}(\chi_1 + \chi_2)e^{-i(\omega_2-\Omega+\delta)t} & \omega_2 + \Omega & 0 \\ \frac{1}{\sqrt{2}}(\chi_1 - \chi_2)e^{-i(\omega_2-\Omega+\delta)t} & 0 & \omega_2 - \Omega \end{pmatrix}. \tag{S7}$$

We denote the dressed state with energy $\omega_2 + \Omega$ as $|d_1\rangle$, and the dressed state with energy $\omega_2 - \Omega$ as $|d_2\rangle$. We can see that if we fine-tune $\chi_1 = -\chi_2$, we synthesize a selection rule where only the transition between $|d_2\rangle$ and $|g\rangle$ is allowed. The synthetic Rabi frequency is then $\sqrt{2}\chi_1$.

This synthetic selection rule can be understood by considering two separate rotating frames with respect to states $|s_1\rangle$ and $|s_2\rangle$, as shown in FIG. S1. In each rotating frame, we have dressed states $|d_1\rangle$ and $|d_2\rangle$. We can couple $|g\rangle$ to dressed states either by driving $|g\rangle$ to dressed states in the $|s_1\rangle$ rotating frame or in the $|s_2\rangle$ rotating frame. By creating interference between the two channels, we obtain a synthetic selection rule.

III. THE CONTINUOUS MERA CIRCUIT ENGINEERING

In this section, we show that by using the scheme shown in FIG. S2(b), we can engineer the disentangler in the interaction picture. Here, we choose the two hyperfine ground states of ^{171}Yb shown in FIG. S3 as our spinor basis of the Chern insulator and effectively couple them to some dressed excited states by two pairs of driving fields. The

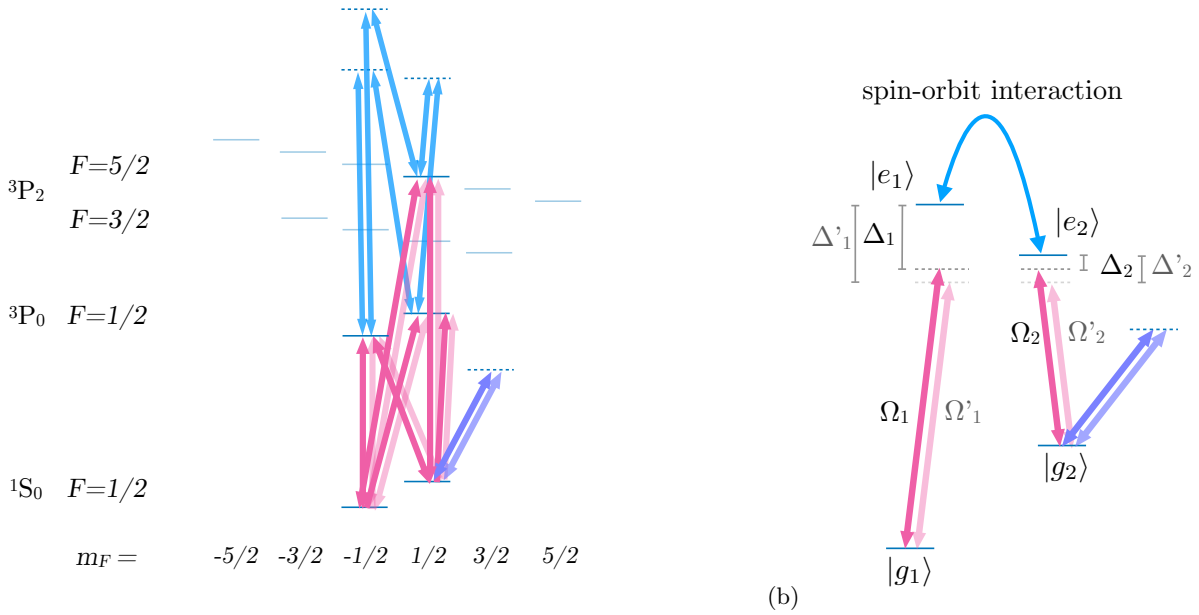

FIG. S2. Disentangler engineering. (a) A magnetic field is applied to induce hyperfine splittings. The excited states are coupled by Raman beams (colored in blue) to generate an effective spin-orbit interaction. They are chosen from the hyperfine manifolds $^3\mathrm{P}_2$ $F = 5/2$ and $^3\mathrm{P}_0$ $F = 1/2$, which are long-lived to circumvent dissipation issues. Their ultra-narrow linewidths are on the order of tens of millihertz [S3–S7]. Additionally, we also have two sets of multiple lasers, colored in light and dark pink, coupling the ground states to the excited states to engineer the disentangler of our cMERA by creating synthetic selection rules. (b) The effective couplings between ground states and the dressed excited states are generated from the scheme shown in (a). We ignore a third dressed state since it is far off-resonant. Now we effectively create two dressed excited states coupled by spin-orbit interaction, which are coupled to the ground states by two pairs of drivings colored in light and dark pink. The synthetic selection rules forbid $|g_1, \mathbf{k}\rangle \longleftrightarrow |e_2, \mathbf{k}\rangle$ and $|g_2, \mathbf{k}\rangle \longleftrightarrow |e_1, \mathbf{k}\rangle$. The effective Rabi frequencies and detunings for two pairs of effective drivings are labeled by unprimed and primed notation. The band structures are ignored in this picture, so by detunings we mean the detunings at $\mathbf{k} = 0$. The light and dark purple arrows on the bottom right in (a) and (b) both represent lasers used to cancel unwanted AC Stark shifts by coupling the ground states to some negative curvature bands of some excited state, e.g., an unused excited state in the $^3\mathrm{P}_2$ $F = 5/2$ hyperfine manifold.

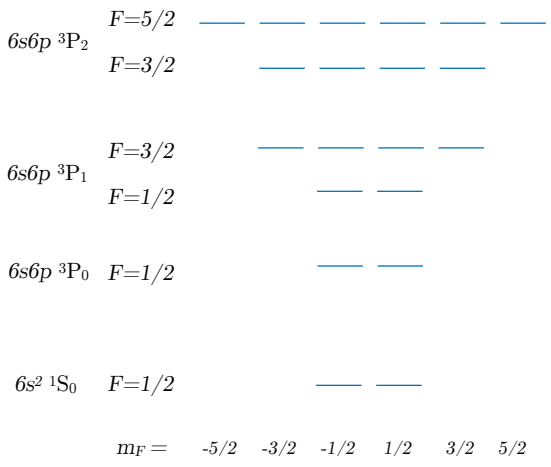

FIG. S3. Energy level diagram of neutral atom ^{171}Yb. The hyperfine structure is shown. We employ the bottom two ground states as our spinor basis of the Chern insulator.

meaning of "dressed" excited states will become clear shortly. Additionally, the dressed excited states are coupled by spin-orbit interaction, while transitions $|g_1,\mathbf{k}\rangle \longleftrightarrow |e_2,\mathbf{k}\rangle$ and $|g_2,\mathbf{k}\rangle \longleftrightarrow |e_1,\mathbf{k}\rangle$ are forbidden. In order to implement this idea in neutral ^{171}Yb atoms, we need to use techniques introduced in Refs. [S8, S9] and Section II. To create states coupled by spin-orbit coupling, we will utilize the method discussed in Refs. [S8, S9]. However, the dressed states created by that scheme do not have good quantum numbers to enforce selection rules. Therefore, we use the technique outlined in Section II to create a synthetic selection rule. In this part of the Supplemental Material, we show how to combine those techniques consistently in neutral ^{171}Yb.

First, we show how FIG. S2(b) arises from FIG. S2(a), inducing the disentangler interaction. We first consider the case with the set of lasers colored in dark pink in FIG. S2(a) with additional Raman lasers coupling the bare excited states. This will give rise to the effective unprimed pair of drivings in FIG. S2(b). We will find that this scheme generates one term in our disentangler with $\mathcal{H}(k)$ described by Eq. (10) in the main text. Therefore, to produce another term, we will use another set of lasers with different parameters, which will effectively induce the primed pair of drivings in FIG. S2(b).

We assume that states $|g_1\rangle$ and $|g_2\rangle$ have flat bands, whereas the chosen bare excited states are weakly trapped. In the continuum, low-energy limit, atoms in the bare excited states can be described by non-relativistic particles with mass M. After appropriate Raman transitions for the bare excited states, we obtain the effective Hamiltonian in the rotating frame of the basis $|g_1\rangle$, $|g_2\rangle$, $|e_{\text{bare},1}\rangle$, $|e_{\text{bare},2}\rangle$, and $|e_{\text{bare},3}\rangle$ under the rotating wave approximation:

$$h = \begin{pmatrix} 0 & 0 & \chi_{1,1}^* e^{i\Delta t} & \chi_{1,2}^* e^{i\Delta t} & \chi_{1,3}^* e^{i\Delta t} \\ 0 & 0 & \chi_{2,1}^* e^{i\Delta t} & \chi_{2,2}^* e^{i\Delta t} & \chi_{2,3}^* e^{i\Delta t} \\ \chi_{1,1} e^{-i\Delta t} & \chi_{2,1} e^{-i\Delta t} & \frac{(\mathbf{k}+\mathbf{k}_1)^2}{2M} & \Omega e^{i\phi_{1,2}} & \Omega e^{-i\phi_{3,1}} \\ \chi_{1,2} e^{-i\Delta t} & \chi_{2,2} e^{-i\Delta t} & \Omega e^{-i\phi_{1,2}} & \frac{(\mathbf{k}+\mathbf{k}_2)^2}{2M} & \Omega e^{i\phi_{2,3}} \\ \chi_{1,3} e^{-i\Delta t} & \chi_{2,3} e^{-i\Delta t} & \Omega e^{i\phi_{3,1}} & \Omega e^{-i\phi_{2,3}} & \frac{(\mathbf{k}+\mathbf{k}_3)^2}{2M} \end{pmatrix}. \tag{S8}$$

The order of the columns is $|g_1,\mathbf{k}\rangle$, $|g_2,\mathbf{k}\rangle$ $|e_{\text{bare},1},\mathbf{k}+\mathbf{k}_1\rangle$, $|e_{\text{bare},2},\mathbf{k}+\mathbf{k}_2\rangle$, and $|e_{\text{bare},3},\mathbf{k}+\mathbf{k}_3\rangle$. The notation Δ is the common detuning of all the lasers coupling the two ground states to the excited states, whereas $\chi_{i,j}$ represents the Rabi frequencies of those lasers. We define the detuning at the zero momentum energy of the bare excited state. Here, $\mathbf{k}_1$, $\mathbf{k}_2$, and $\mathbf{k}_3$ are subject to the condition $|k_1| = |k_2| = |k_3| = k_{\text{SOC}}$, $\mathbf{k}_1+\mathbf{k}_2+\mathbf{k}_3 = 0$, and $\mathbf{k}_j = k_{\text{SOC}}[\cos(2\pi j/3)\mathbf{e}_x + \sin(2\pi j/3)\mathbf{e}_y]$.

We apply the following unitaries to conjugate the single body Hamiltonian

$$U = \begin{pmatrix} 1 & 0 & 0 & 0 & 0 \\ 0 & 1 & 0 & 0 & 0 \\ 0 & 0 & e^{-i2\pi/3}/\sqrt{3} & e^{-i4\pi/3}/\sqrt{3} & 1/\sqrt{3} \\ 0 & 0 & e^{-i4\pi/3}/\sqrt{3} & e^{-i8\pi/3}/\sqrt{3} & 1/\sqrt{3} \\ 0 & 0 & s1/\sqrt{3} & 1/\sqrt{3} & 1/\sqrt{3} \end{pmatrix}, \tag{S9}$$

$$U' = \begin{pmatrix} 1 & 0 & 0 & 0 & 0 \\ 0 & 1 & 0 & 0 & 0 \\ 0 & 0 & e^{i(\phi_{1,2}+\phi_{2,3}+\phi_{3,1})/3} & 0 & 0 \\ 0 & 0 & 0 & e^{i(-\phi_{1,2}+2\phi_{2,3}+2\phi_{3,1})/3} & 0 \\ 0 & 0 & 0 & 0 & e^{i\phi_{3,1}} \end{pmatrix}, \tag{S10}$$

and assume the following to obtain a synthetic selection rule:

$$\begin{aligned} \chi_{1,2} &= e^{2\pi i/3} e^{-i(2\phi_{1,2}-\phi_{2,3}-\phi_{3,1})/3} \chi_{1,1} \\ \chi_{1,3} &= e^{-2\pi i/3} e^{-i(\phi_{1,2}+\phi_{2,3}-2\phi_{3,1})/3} \chi_{1,1} \\ \chi_{2,1} &= e^{2\pi i/3} e^{i(2\phi_{1,2}-\phi_{2,3}-\phi_{3,1})/3} \chi_{2,2} \\ \chi_{2,3} &= e^{-2\pi i/3} e^{i(\phi_{1,2}-2\phi_{2,3}+\phi_{3,1})/3} \chi_{2,2}. \end{aligned} \tag{S11}$$

The Hamiltonian becomes

$$(U'U)^\dagger hU'U = \begin{pmatrix} 0 & 0 & \Omega_1^* e^{i\Delta t} & 0 & 0 \\ 0 & 0 & 0 & \Omega_2^* e^{i\Delta t} & 0 \\ \Omega_1 e^{-i\Delta t} & 0 & \frac{k^2+k_{\mathrm{SOC}}^2}{2M} + 2\Omega\cos(\frac{2\pi}{3}-\phi) & \frac{k_{\mathrm{SOC}}}{M}(k_x - ik_y) & \frac{k_{\mathrm{SOC}}}{M}(k_x + ik_y) \\ 0 & \Omega_2 e^{-i\Delta t} & \frac{k_{\mathrm{SOC}}}{M}(k_x + ik_y) & \frac{k^2+k_{\mathrm{SOC}}^2}{2M} + 2\Omega\cos(\frac{4\pi}{3}-\phi) & \frac{k_{\mathrm{SOC}}}{M}(k_x - ik_y) \\ 0 & 0 & \frac{k_{\mathrm{SOC}}}{M}(k_x - ik_y) & \frac{k_{\mathrm{SOC}}}{M}(k_x + ik_y) & \frac{k^2+k_{\mathrm{SOC}}^2}{2M} + 2\Omega\cos(\phi) \end{pmatrix}, \tag{S12}$$

where $\Omega_1 \equiv -\sqrt{3}e^{-i\pi/3}e^{-i(\phi_{1,2}+\phi_{2,3}+\phi_{3,1})/3}\chi_{1,1}$, $\Omega_2 \equiv -\sqrt{3}e^{-i\pi/3}e^{i(\phi_{1,2}-2\phi_{2,3}-2\phi_{3,1})/3}\chi_{2,2}$, and $\phi \equiv (\phi_{1,2}+\phi_{2,3}+\phi_{3,1})/3$. The order of the columns is $|g_1,\mathbf{k}\rangle$, $|g_2,\mathbf{k}\rangle$, $|e_1,\mathbf{k}\rangle$, $|e_2,\mathbf{k}\rangle$, and $|e_3,\mathbf{k}\rangle$. States $|e_1,\mathbf{k}\rangle$, $|e_2,\mathbf{k}\rangle$, $|e_3,\mathbf{k}\rangle$ are dressed excited states which are linear combinations of the bare excited states $|e_{\mathrm{bare},1},\mathbf{k}+\mathbf{k}_1\rangle$, $|e_{\mathrm{bare},2},\mathbf{k}+\mathbf{k}_2\rangle$, and $|e_{\mathrm{bare},3},\mathbf{k}+\mathbf{k}_3\rangle$. By adiabatically eliminating the dressed excited state representing the third column (row) to the zeroth order and expanding ϕ to the first order, we obtain the effective Hamiltonian

$$\begin{pmatrix} 0 & 0 & \Omega_1^* e^{i\Delta t} & 0 \\ 0 & 0 & 0 & \Omega_2^* e^{i\Delta t} \\ \Omega_1 e^{-i\Delta t} & 0 & \frac{k^2}{2M} + E_{\mathrm{SOC}} + \sqrt{3}\Omega\phi & \frac{k_{\mathrm{SOC}}}{M}(k_x - ik_y) \\ 0 & \Omega_2 e^{-i\Delta t} & \frac{k_{\mathrm{SOC}}}{M}(k_x + ik_y) & \frac{k^2}{2M} + E_{\mathrm{SOC}} - \sqrt{3}\Omega\phi \end{pmatrix}, \tag{S13}$$

where $E_{\mathrm{SOC}} \equiv k_{\mathrm{SOC}}^2/2M - \Omega$. The order of the columns is $|g_1,\mathbf{k}\rangle$, $|g_2,\mathbf{k}\rangle$, $|e_1,\mathbf{k}\rangle$, and $|e_2,\mathbf{k}\rangle$. By inspecting the matrix elements, one can see that a spin-orbit interaction and a synthetic selection rule shown in FIG. S2(b) have been consistently generated as we claimed.

Now, we are going to show that with this Hamiltonian, we can almost generate the disentangler. First, we go to a frame in which $|e_1,\mathbf{k}\rangle$ and $|e_2,\mathbf{k}\rangle$ rotate with frequency Δ. The Hamiltonian becomes

$$\begin{pmatrix} 0 & 0 & \Omega_1^* & 0 \\ 0 & 0 & 0 & \Omega_2^* \\ \Omega_1 & 0 & \frac{k^2}{2M} + E_{\mathrm{SOC}} - \Delta + \sqrt{3}\Omega\phi & \frac{k_{\mathrm{SOC}}}{M}(k_x - ik_y) \\ 0 & \Omega_2 & \frac{k_{\mathrm{SOC}}}{M}(k_x + ik_y) & \frac{k^2}{2M} + E_{\mathrm{SOC}} - \Delta - \sqrt{3}\Omega\phi \end{pmatrix}. \tag{S14}$$

For the sake of later convenience, we denote $\Delta_1 \equiv E_{\mathrm{SOC}} - \Delta + \sqrt{3}\Omega\phi$ and $\Delta_2 \equiv E_{\mathrm{SOC}} - \Delta - \sqrt{3}\Omega\phi$:

$$\begin{pmatrix} 0 & 0 & \Omega_1^* & 0 \\ 0 & 0 & 0 & \Omega_2^* \\ \Omega_1 & 0 & \Delta_1 + k^2/2M & \frac{k_{\mathrm{SOC}}}{M}(k_x - ik_y) \\ 0 & \Omega_2 & \frac{k_{\mathrm{SOC}}}{M}(k_x + ik_y) & \Delta_2 + k^2/2M \end{pmatrix}. \tag{S15}$$

We can see that Δ_1 and Δ_2 correspond to the effective detunings at $\mathbf{k} = 0$. Define $\alpha = k_{\mathrm{SOC}}/M$ and k, $\theta_{\mathbf{k}}$ such that $k\cos\theta_{\mathbf{k}} = k_x$ and $k\sin\theta_{\mathbf{k}} = k_y$ to simplify our calculations. Notice that we have chosen a different sign convention of the detunings Δ_1 and Δ_2 from the normal convention. We will assume that $\Delta_1, \Delta_2 > 0$ in our system so that the effective drivings are red-detuned. Now we conjugate the Hamiltonian with the following unitary matrix:

$$\begin{pmatrix} 1 & 0 & 0 & 0 \\ 0 & 1 & 0 & 0 \\ 0 & 0 & 1 - \frac{\alpha^2 k^2}{2(\Delta_1-\Delta_2)^2} & -\frac{\alpha k e^{-i\theta_{\mathbf{k}}}}{\Delta_1-\Delta_2} \\ 0 & 0 & \frac{\alpha k e^{i\theta_{\mathbf{k}}}}{\Delta_1-\Delta_2} & 1 - \frac{\alpha^2 k^2}{2(\Delta_1-\Delta_2)^2} \end{pmatrix} + O\left(\left(\frac{\alpha k}{\Delta_1-\Delta_2}\right)^3\right), \tag{S16}$$

and the effective Hamiltonian to order $\left(\frac{\alpha k}{\Delta_1-\Delta_2}\right)^3$ becomes

$$\begin{pmatrix} 0 & 0 & \Omega_1^*\left(1 - \frac{\alpha^2 k^2}{2(\Delta_1-\Delta_2)^2}\right) & -\frac{\Omega_1^* \alpha k e^{-i\theta_{\mathbf{k}}}}{\Delta_1-\Delta_2} \\ 0 & 0 & \frac{\Omega_2^* \alpha k e^{i\theta_{\mathbf{k}}}}{\Delta_1-\Delta_2} & \Omega_2^*\left(1 - \frac{\alpha^2 k^2}{2(\Delta_1-\Delta_2)^2}\right) \\ \Omega_1\left(1 - \frac{\alpha^2 k^2}{2(\Delta_1-\Delta_2)^2}\right) & \frac{\Omega_2 \alpha k e^{-i\theta_{\mathbf{k}}}}{\Delta_1-\Delta_2} & \Delta_1 + \frac{\alpha^2 k^2}{\Delta_1-\Delta_2} + k^2/2M & 0 \\ -\frac{\Omega_1 \alpha k e^{i\theta_{\mathbf{k}}}}{\Delta_1-\Delta_2} & \Omega_2\left(1 - \frac{\alpha^2 k^2}{2(\Delta_1-\Delta_2)^2}\right) & 0 & \Delta_2 - \frac{\alpha^2 k^2}{\Delta_1-\Delta_2} + k^2/2M \end{pmatrix}. \tag{S17}$$

If we assume that $M \gg \frac{k_{\mathrm{SOC}}^2}{\Delta_1-\Delta_2}$, we can ignore the terms $\frac{\alpha^2 k^2}{\Delta_1-\Delta_2}$ in the $(3,3)$ and $(4,4)$ entries. Now, we also drop $O\left(\left(\frac{\alpha k}{\Delta_1-\Delta_2}\right)^2\right)$ terms in the $(1,3)$, $(2,4)$, $(3,1)$, and $(4,2)$ entries. The remaining Hamiltonian is

$$\begin{pmatrix} 0 & 0 & \Omega_1^* & -\frac{\Omega_1^* \alpha k e^{-i\theta_{\mathbf{k}}}}{\Delta_1-\Delta_2} \\ 0 & 0 & \frac{\Omega_2^* \alpha k e^{i\theta_{\mathbf{k}}}}{\Delta_1-\Delta_2} & \Omega_2^* \\ \Omega_1 & \frac{\Omega_2 \alpha k e^{-i\theta_{\mathbf{k}}}}{\Delta_1-\Delta_2} & \Delta_1 + k^2/2M & 0 \\ -\frac{\Omega_1 \alpha k e^{i\theta_{\mathbf{k}}}}{\Delta_1-\Delta_2} & \Omega_2 & 0 & \Delta_2 + k^2/2M \end{pmatrix}. \tag{S18}$$

We adiabatically eliminate the state in the first and second columns (rows). The remaining Hamiltonian of the subspace spanned by dressed states $|\tilde{g}_1, \mathbf{k}\rangle$, and $|\tilde{g}_2, \mathbf{k}\rangle$ is

$$\begin{pmatrix} -\frac{|\Omega_1|^2}{\Delta_1+k^2/2M} - \frac{|\Omega_1|^2}{\Delta_2+k^2/2M}\left(\frac{\alpha k}{\Delta_1-\Delta_2}\right)^2 & \frac{\alpha k e^{-i\theta_{\mathbf{k}}} \Omega_1^* \Omega_2}{(\Delta_1-\Delta_2)(\Delta_1+k^2/2M)} - \frac{\alpha k e^{-i\theta_{\mathbf{k}}} \Omega_1^* \Omega_2}{(\Delta_1-\Delta_2)(\Delta_2+k^2/2M)} \\ \frac{\alpha k e^{i\theta_{\mathbf{k}}} \Omega_1 \Omega_2^*}{(\Delta_1-\Delta_2)(\Delta_1+k^2/2M)} - \frac{\alpha k e^{i\theta_{\mathbf{k}}} \Omega_1 \Omega_2^*}{(\Delta_1-\Delta_2)(\Delta_2+k^2/2M)} & -\frac{|\Omega_2|^2}{\Delta_1+k^2/2M}\left(\frac{\alpha k}{\Delta_1-\Delta_2}\right)^2 - \frac{|\Omega_2|^2}{\Delta_2+k^2/2M} \end{pmatrix}. \tag{S19}$$

We have assumed $\Delta_1, \Delta_2, \gg \Omega_1, \Omega_2$. A necessary condition of this assumption is that $\Omega \gg \Omega_1, \Omega_2$. Now, supposing that we can tune $\Delta_1 \gg \Delta_2$, and that the region of the Brillouin zone we consider satisfies $\Delta_1 \gg k^2/2M$, by dropping terms to quadratic order in $\frac{\alpha k}{\Delta_1-\Delta_2}$, we obtain the Hamiltonian

$$\begin{pmatrix} 0 & -\frac{\alpha k e^{-i\theta_{\mathbf{k}}} \Omega_1^* \Omega_2}{\Delta_1(\Delta_2+k^2/2M)} \\ -\frac{\alpha k e^{i\theta_{\mathbf{k}}} \Omega_1 \Omega_2^*}{\Delta_1(\Delta_2+k^2/2M)} & -\frac{|\Omega_2|^2}{\Delta_2+k^2/2M} \end{pmatrix}. \tag{S20}$$

To make this approximation, we have assumed that the off-diagonal elements of Eq. (S20) are much greater than the terms in Eq. (S19) being dropped in Eq. (S20). There is a mismatch between the diagonal elements. To make states $|\tilde{g}_1, \mathbf{k}\rangle$ and $|\tilde{g}_2, \mathbf{k}\rangle$ rotate at the same speed, we might either couple the state $|\tilde{g}_1, \mathbf{k}\rangle$ to a band with positive curvature to induce an AC Stark shift to cancel the first diagonal entry or couple the state $|\tilde{g}_2, \mathbf{k}\rangle$ to some band with negative curvature to induce an AC Stark shift to cancel the second diagonal entry. The curvatures of those auxiliary bands have to be tuned properly during the whole process.

Now, we have engineered one term in our disentangler with $\mathcal{H}(k)$ described by Eq. (10). We can choose a different Ω_1', Ω_2', Δ_1', Δ_2' to generate the second term. We have to assume that the beat note between the two schemes satisfies $|\Delta_2 - \Delta_2'| \gg \left|\frac{\alpha k e^{-i\theta_{\mathbf{k}}} \Omega_1^* \Omega_2}{\Delta_1(\Delta_2+k^2/2M)}\right|, \left|\frac{\alpha k e^{-i\theta_{\mathbf{k}}} \Omega'^*_1 \Omega'_2}{\Delta_1'(\Delta_2'+k^2/2M)}\right|$ to avoid crosstalk. Applying both of them at the same time, we have the Hamiltonian in the $|\tilde{g}_1, \mathbf{k}\rangle$, $|\tilde{g}_2, \mathbf{k}\rangle$ basis:

$$\begin{pmatrix} 0 & -\frac{\alpha k e^{-i\theta_{\mathbf{k}}} \Omega_1^* \Omega_2}{\Delta_1(\Delta_2+k^2/2M)} - \frac{\alpha k e^{-i\theta_{\mathbf{k}}} \Omega'^*_2}{\Delta_1'(\Delta_2'+k^2/2M)} \\ -\frac{\alpha k e^{i\theta_{\mathbf{k}}} \Omega_1 \Omega_2^*}{\Delta_1(\Delta_2+k^2/2M)} - \frac{\alpha k e^{i\theta_{\mathbf{k}}} \Omega'_1 \Omega'^*_2}{\Delta_1'(\Delta_2'+k^2/2M)} & 0 \end{pmatrix}. \tag{S21}$$

Now we list all the assumptions that have been made:

1. The energy splittings of the dressed excited states, which are of order Ω, have to be much smaller than the hyperfine splittings of all the states that we used. Otherwise, in FIG. S2(a), we cannot use frequency selection to control each transition to engineer synthetic selection rules.

2. All the momentum kicks should allow atoms to be in the same Brillouin zone so that the continuum limit applies. That is, $k_{\mathrm{SOC}}\, a \ll 1$, where a is the optical lattice constant.

3. $\frac{\alpha k}{\Delta_1-\Delta_2} = \frac{k_{\mathrm{SOC}} k}{M(\Delta_1-\Delta_2)} \ll 1$ and $\frac{k_{\mathrm{SOC}}^2}{M(\Delta_1-\Delta_2)} \ll 1$ as well as the primed version.

4. $\Delta_1 \gg \Delta_2$, $k^2/2M$ as well as the primed version.

5. Δ_1, $\Delta_2 \gg \Omega_1$, Ω_2 and Δ_1', $\Delta_2' \gg \Omega_1'$, Ω_2'. These two conditions imply that $\Omega \gg \Omega_1$, Ω_2, Ω_1', Ω_2'.

6. The off-diagonal elements of Eq. (S20) are much greater than the terms in Eq. (S19) being dropped in Eq. (S20).

7. $|\Delta_2 - \Delta_2'| \gg \left|\frac{\alpha k e^{-i\theta_{\mathbf{k}}} \Omega_1^* \Omega_2}{\Delta_1(\Delta_2+k^2/2M)}\right|, \left|\frac{\alpha k e^{-i\theta_{\mathbf{k}}} \Omega'^*_1 \Omega'_2}{\Delta_1'(\Delta_2'+k^2/2M)}\right|$ to avoid crosstalk between the scheme determined by Ω_1, Ω_2, Δ_1, Δ_2 and the scheme determined by Ω_1', Ω_2', Δ_1', Δ_2'.

We remind the readers that we engineer the cMERA circuit entirely in the interaction picture; therefore, the action of the isometry is absorbed into that of the disentangler. The price that we have to pay is that the disentangler is not scale-invariant at all in the interaction picture. In principle, one can also engineer the cMERA circuit in the Schrödinger picture. We leave this as a question for future research.

IV. PREPARATION OF THE INITIAL NEAR-IR STATE

The near-IR state with a large but finite negative u is described by Eq. (9). We imagine the state to be infrared enough that the Berry curvature is concentrated on a few momentum points near $k = 0$. Here, we describe how it can be created to use as input to the MERA circuit. A strong magnetic field should be applied to induce hyperfine splitting in the ground-state manifold. We start with all states in the $|g_1\rangle$ state, which is easy to prepare by dissipation techniques. We then use a long-lived clock state $^3\mathrm{P}_0$ $|F = 1/2,\, m_F = 1/2\rangle$ [S3–S6] as a "bus" state $|e\rangle$ to transfer amplitude from $|g_1\rangle$ to $|g_2\rangle$. Seeing that S states and P states are well separated, we can use a two-dimensional optical lattice to tightly trap atoms in the S states and let the atoms in the P states propagate nearly freely. We assume that the z direction is tightly confined for all states, so the corresponding degrees of freedom can be ignored. The energy bands of $|g_1\rangle$ and $|g_2\rangle$ are flat. Here, we assume that the $|e\rangle$ state is highly stable with a natural linewidth much smaller than the energy splitting between the spatial ground state and the first spatial excited state, allowing individual momentum states to be resolved and manipulated.

In the following, we are going to use the spatial ground state of $|e\rangle$ as a bus state. Due to open boundary conditions of optical lattices, the Bloch waves are no longer energy eigenstates for the excited state $|e\rangle$ and we must use standing waves instead. Note that since the eigenstates in position space of the hyperfine ground states $|g_1\rangle$ and $|g_2\rangle$ are tightly trapped and highly degenerate, we can still make superpositions of standing waves to create Bloch waves as energy eigenstates. Intuitively, since particles in the hyperfine ground states $|g_1\rangle$ and $|g_2\rangle$ are tightly trapped, particles far from the boundary cannot distinguish between different boundary conditions. Our procedure to prepare the IR state is to transfer partial amplitude from state $|g_1\rangle$ to $|g_2\rangle$ in the Brillouin zone for each $\mathbf{k}$. We denote the lowest energy point of $|e\rangle$ as $|e, 0\rangle$, which is a standing wave with small amplitude on the boundary. We couple that state resonantly to $|g_1, \mathbf{k}\rangle$ and $|g_2, \mathbf{k}\rangle$ successively by different light fields, i.e., $|g_1, \mathbf{k}\rangle \longleftrightarrow |e, 0\rangle$ and then $|e, 0\rangle \longleftrightarrow |g_2, \mathbf{k}\rangle$. Other standing waves of $|e\rangle$ are decoupled from the process due to driving frequency mismatch. Here, we also need to ensure that other states $|g_1, \mathbf{k}'\rangle$ and $|g_2, \mathbf{k}'\rangle$ with different momenta do not interfere with the process. As a consequence, the light fields must create a momentum selection rule for the transitions $|g_1, \mathbf{k}\rangle \longleftrightarrow |e, 0\rangle$ and $|e, 0\rangle \longleftrightarrow |g_2, \mathbf{k}\rangle$.

We imagine a square well with wavefunction amplitude vanishing on the periphery. This can be done by tuning the potential with spatial light modulators [S1, S2]. In the following, we work in the basis of the Wannier functions of the ground states and the excited state, modeling the system by a $N+2$ by $N+2$ square lattice. We can label the lattice points by the vector $\mathbf{x} = (x_1,\, x_2)$, where $0 \le x_1,\, x_2 \le N+1$, while the wavefunction vanishes at points with $x_1 = 0,\, N+1$ or $x_2 = 0,\, N+1$. Therefore, the active degrees of freedom for the hyperfine ground states $|g_1\rangle$ and $|g_2\rangle$ will be at $1 \le x_1,\, x_2 \le N$. In this case, the unnormalized single-particle wavefunction of the ground state $|g_1, \mathbf{k}\rangle$ is [S10]

$$\psi_{g_1}(\mathbf{x}) = \langle \mathbf{x} | g_1, \mathbf{k}\rangle = \exp\left(i\,\mathbf{k}\cdot\mathbf{x}\right), \tag{S22}$$

where $\mathbf{k} = 2\pi\left(n_1,\, n_2\right)/N$ with $n_1, n_2 \in \{n \mid n \in \mathbb{Z}, -N/2 < n \le N/2\}$, and $1 \le x_1,\, x_2 \le N$. The counterpart for the excited state $|e\rangle$ is

$$\psi_e(\mathbf{x}) = \langle \mathbf{x} | e, 0\rangle = \sin\left(\frac{\pi}{N+1}x_1\right)\sin\left(\frac{\pi}{N+1}x_2\right). \tag{S23}$$

Using spatial light modulators [S1, S2], we create the following light field:

$$E_{g_1}(\mathbf{x}) = \frac{\exp\left(-i\,\mathbf{q}\cdot\mathbf{x}\right)}{\sin\left(\frac{\pi}{N+1}x_1\right)\sin\left(\frac{\pi}{N+1}x_2\right)}, \tag{S24}$$

where $\mathbf{q} = 2\pi\left(m_1,\, m_2\right)/N,\ m_1, m_2 \in \mathbb{Z}$. A momentum selection rule for $|g_1, \mathbf{k}\rangle \longleftrightarrow |e, 0\rangle$ can now be engineered:

$$\begin{aligned}\sum_{\mathbf{x}} \psi_e(\mathbf{x})\, E_{g_1}(\mathbf{x})\, \psi_{g_1}(\mathbf{x}) &= \sum_{\mathbf{x}} \sin\left(\frac{\pi}{N+1}x_1\right)\sin\left(\frac{\pi}{N+1}x_2\right)\frac{\exp\left(-i\,\mathbf{q}\cdot\mathbf{x}\right)}{\sin\left(\frac{\pi}{N+1}x\right)\sin\left(\frac{\pi}{N+1}x_2\right)}\exp\left(i\,\mathbf{k}\cdot\mathbf{x}\right) \\ &= \sum_{\mathbf{x}} \exp\left(i\left(\mathbf{k}-\mathbf{q}\right)\cdot\mathbf{x}\right) \propto \delta_{\mathbf{k},\mathbf{q}}.\end{aligned} \tag{S25}$$

Notice that since the points where the denominator of $E(\mathbf{x})$ becomes zero are excluded from our consideration, the light field is well defined. A similar selection rule can be derived for $|e,0\rangle \longleftrightarrow |g_2,\mathbf{k}\rangle$.

With this technique in mind, we can adjust the relative amplitude between $|g_1\rangle$ and $|g_2\rangle$ in the Brillouin zone to create the near-IR state described in Eq. (9) by fine-tuning phases and durations of the light field pulses. Given that the Berry curvature is concentrated on a few momentum points near $k = 0$, we can limit this procedure to only a few small momentum points without too much error.

[S1] T. Fukuhara, A. Kantian, M. Endres, M. Cheneau, P. Schauß, S. Hild, D. Bellem, U. Schollwöck, T. Giamarchi, C. Gross, I. Bloch, and S. Kuhr, "Quantum dynamics of a mobile spin impurity," Nat. Phys. **9**, 235 EP – (2013).

[S2] F. Nogrette, H. Labuhn, S. Ravets, D. Barredo, L. Béguin, A. Vernier, T. Lahaye, and A. Browaeys, "Single-atom trapping in holographic 2d arrays of microtraps with arbitrary geometries," Phys. Rev. X **4**, 021034 (2014).

[S3] X. Zhang, M. Zhou, N. Chen, Q. Gao, C. Han, Y. Yao, P. Xu, S. Li, Y. Xu, Y. Jiang, Z. Bi, L. Ma, and X. Xu, "Study on the clock-transition spectrum of cold 171 Yb ytterbium atoms," Laser Phys. Lett. **12**, 25501 (2015).

[S4] T. Kohno, M. Yasuda, K. Hosaka, H. Inaba, Y. Nakajima, and F.-L. Hong, "One-Dimensional Optical Lattice Clock with a Fermionic 171 Yb Isotope," Appl. Phys. Express **2**, 072501 (2009).

[S5] N. D. Lemke, A. D. Ludlow, Z. W. Barber, T. M. Fortier, S. A. Diddams, Y. Jiang, S. R. Jefferts, T. P. Heavner, T. E. Parker, and C. W. Oates, "Spin-1/2 optical lattice clock," Phys. Rev. Lett. **103**, 063001 (2009).

[S6] C. Y. Park, D.-H. Yu, W.-K. Lee, S. E. Park, E. B. Kim, S. K. Lee, J. W. Cho, T. H. Yoon, J. Mun, S. J. Park, T. Y. Kwon, and S.-B. Lee, "Absolute frequency measurement of transition of ^{1}S$_0$(F=1/2)-^{3}P$_0$(F=1/2) ^{171}Yb atoms in a one-dimensional optical lattice at KRISS," Metrologia **50**, 119–128 (2013).

[S7] A. Yamaguchi, *Metastable State of Ultracold and Quantum Degenerate Ytterbium Atoms: High-Resolution Spectroscopy and Cold Collisions*, Ph.D. thesis, Kyoto University (2008).

[S8] D. L. Campbell, G. Juzeliunas, and I. B. Spielman, "Realistic Rashba and Dresselhaus spin-orbit coupling for neutral atoms," Phys. Rev. A **84**, 025602 (2011).

[S9] D. L. Campbell and I. B. Spielman, "Rashba realization: Raman with RF," New J. Phys. **18**, 033035 (2016).

[S10] U. Busch and K. A. Penson, "Tight-binding electrons on open chains: Density distribution and correlations," Phys. Rev. B **36**, 9271–9274 (1987).